RS•C

$CH_3OH \longrightarrow$
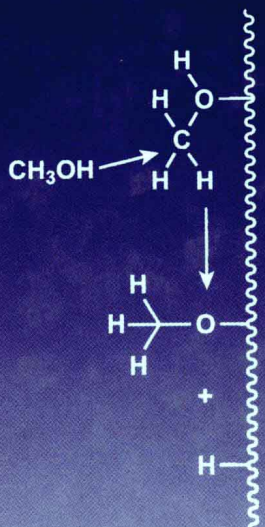
Catalysis

Volume 18

senior reporter J.J. SPIVEY

If you buy this title on standing order, you will be given FREE access to the chapters online. Please contact sales@rsc.org with proof of purchase to arrange access to be set up.

Thank you.

Preface

The application of catalytic principles to energy and chemical production as well as the challenges of environmental issues remains an important field of study. There continue to be new ideas, new problems to be solved, and new insight into how catalysts work. It is my hope that this volume of the Catalysis book series will be a resource for those who are working in this exciting area.

This volume consists of reviews devoted to a range of important subjects. Vadim Guliants and Moises Carreon (University of Cincinnati) review the selective oxidation of butane. This is an excellent example of a catalytic process designed to add value to an inexpensive raw material, and is the only vapor phase selective oxidation of an alkane that is practiced industrially. This process also avoids the use of benzene, which eliminates the risk of handling this carcinogenic compound. The authors review the synthesis, activation, and mechanism of this reaction on V-P-O catalysts.

Gabriele Centi and Siglinda Perathoner (University of Messina, Italy) examine the use of solid catalysts for the removal of contaminants from water supplies. This includes photocatalytic processes as well as oxidation and reduction reactions. There are a wide range of catalysts used in these various processes. In addition to their activity, deactivation is often a critical concern. The authors show that there are significant challenges remaining in this area.

The use of polynuclear metal complexes provides a novel approach to the synthesis of supported metals and metal oxides. Mark White (Georgia Tech) shows how these materials can be synthesized and characterized. Quantum mechanics are used to compare predicted and experimental results of the interactions of the metal complexes and surfaces. The use of these materials as both adsorbents and catalysts suggests the importance of understanding both how they are synthesized, and their post-synthesis structure.

In-Sik Nam and Moon Hyeon Kim (Pohang University of Science and Technology, Korea) review new materials for the selective catalytic reduction of NO_x from combustion processes. Despite significant research efforts over the last 20 years, there are still unresolved issues, such as inhibition and deactivation by steam. The authors show how new synthesis methods, especially for zeolites, can be used to improve these catalysts.

Finally, Steve Chuang (University of Akron) reviews catalysts for use in solid oxide fuel cells. These fuel cells hold the promise of significant improvements in energy efficiency with minimum emissions, but challenges remain – particularly for the catalysts. A particular challenge is the effect of the high temperature operation on the oxide electrolyte. Also important is the stability of the anode in

v

the reducing environment and its tolerance to sulfur. These and other constraints on the catalysts used in this fuel cell are the subject of this review.

I wish to thank the authors for the effort they have put into these chapters, and the Royal Society of Chemistry for their support, particularly Janet Freshwater. Comments and suggestions are welcome.

James J. Spivey
Department of Chemical Engineering
Louisiana State University
Baton Rouge, LA 70803
jjspivey@lsu.edu

Contents

1

Vanadium-Phosphorus-Oxides: from Fundamentals of *n*-Butane Oxidation to Synthesis of New Phases

BY VADIM V. GULIANTS AND MOISES A. CARREON

1 Introduction

The abundance and low cost of light alkanes have generated in recent years considerable interest in their oxidative catalytic conversion to olefins, oxygenates and nitriles in the petroleum and petrochemical industries [1-4]. Rough estimates place the annual worth of products that have undergone a catalytic oxidation step at $20-40 billion worldwide [4]. Among these, the 14-electron selective oxidation of *n*-butane to maleic anhydride (2,5-furandione) on vanadium-phosphorus-oxide (VPO) catalysts is one of the most fascinating and unique catalytic processes [4,5]:

$$\text{\includegraphics{butane} } + \ 3.5O_2 \ \longrightarrow \ \text{\includegraphics{maleic anhydride} } + \ 4H_2O$$
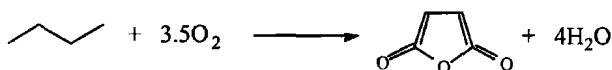
It is the only industrial process of a selective vapor-phase oxidation of an alkane that uses dioxygen [5]. The demand for maleic anhydride comes principally from the manufacture of unsaturated polyester resins, agricultural chemicals, food additives, lubricating oil additives, and pharmaceuticals [6].

Bergman and Frisch [7] disclosed in 1966 that selective oxidation of *n*-butane was catalyzed by the VPO catalysts, and since 1974 *n*-butane has been increasingly used instead of benzene as the raw material for maleic anhydride production due to lower price, high availability in many regions and low environmental impact [8]. At present more than 70 % of maleic anhydride is produced from *n*-butane [6]. However, productivity from *n*-butane is lower than in the case of benzene due to lower selectivities to maleic anhydride at higher conversions and somewhat lower feed concentrations (< 2 mol. %) used to avoid flammability of a process stream. Under typical industrial conditions (2 mol. % *n*-butane in air, 673-723K, and space velocities of 1100-2600 h^{-1}) the selectivities [9] for fixed-bed production of maleic anhydride from *n*-butane are 67-75 mol. % at 70-85 % *n*-butane conversion [10]. Another unique feature of the VPO catalysts is that no support is used in partial oxidation of *n*-butane.Many studies of *n*-butane oxidation on the VPO catalysts indicated that crystalline vanadyl(IV) pyrophos-

phate, $(VO)_2P_2O_7$, is present in the most selective catalysts, e.g. [10-12]. However, the VPO system is characterized by facile formation and interconversion of a number of crystalline and amorphous V^{III}, V^{IV} and V^V phosphates [10]. Various research groups detected these phases in the VPO catalysts and proposed different models of the active and selective VPO phase and surface sites in *n*-butane oxidation [10-13].

The VPO catalysts are prepared by thermal dehydration of its precursor, vanadyl(IV) hydrogen phosphate hemihydrate, $VOHPO_4 \cdot 0.5H_2O$. The catalytic performance of the VPO catalysts depends on (i) the method of $VOHPO_4 \cdot 0.5H_2O$ synthesis (types and concentrations of reagents, reducing agents and solvents, the reduction temperature and synthesis duration), (ii) the procedures for activation and conditioning of the precursor at high temperature and (iii) the nature of metal promoters. These factors important for understanding the catalytic behavior of the VPO system in *n*-butane oxidation were discussed previously in a number of excellent early reviews [10-14]. Therefore, in this chapter we briefly go over the conclusions of early studies and discuss in greater detail recent findings with emphasis on fundamental aspects of VPO catalysis, such as the mechanism of $VOHPO_4 \cdot 0.5H_2O$ formation and its transformation to active and selective VPO catalysts, the mechanism of *n*-butane oxidation, the role of promoters and the synthesis of new VPO phases. It is expected that new fundamental insights into molecular structure and catalytic function of this unique catalytic system will lead to the design of improved mixed metal oxide catalysts for selective oxidation of light alkanes.

2   Synthesis of $VOHPO_4 \cdot 0.5H_2O$ Precursor

There is a general agreement in the VPO literature [4, 10, 14-21] that the necessary synthesis conditions to obtain an optimal catalyst are the following: (i) synthesis of microcrystalline $VOHPO_4 \cdot 0.5H_2O$ in an alcohol characterized by the preferential exposure of the basal (001) planes, (ii) the presence of defects in the stacking of the (001) planes and (iii) a slight excess of phosphate with respect to the stoichiometric amount employed in the synthesis (P/V = 1.01-1.10). This excess phosphate is strongly bound to the surface and cannot be removed by simple washing of the precursor in polar solvents.

Three major synthesis methods were reported for preparation of the $VOHPO_4 \cdot 0.5H_2O$ precursor:

1.   In *aqueous synthesis*, V^V compounds (e.g. V_2O_5) are reduced to V^{IV} in aqueous solutions of orthophosphoric acid, followed by evaporation of the solvent to dryness [22]:

$$V_2O_5 + 2NH_2OH \cdot HCl + 2H_3PO_4 \rightarrow 2VOHPO_4 \cdot 0.5H_2O + N_2$$
$$+ 2HCl + 4H_2O$$
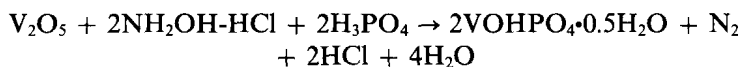
2.   In *organic synthesis*, V^V compounds are reduced by an anhydrous alcohol, followed by the addition of anhydrous orthophosphoric acid dissolved in the same alcohol and precipitation of $VOHPO_4 \cdot 0.5H_2O$ [16, 19]:

$$V_2O_5 + EtCHOHMe + 2H_3PO_4 \rightarrow 2VOHPO_4 \cdot 0.5H_2O + EtCOMe + 2H_2O$$
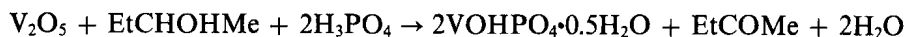
3. In *model organic synthesis*, V^V orthophosphate dihydrate, $VOPO_4 \cdot 2H_2O$, is first synthesized from V_2O_5 and H_3PO_4 in aqueous medium and then reduced to $VOHPO_4 \cdot 0.5H_2O$ by an alcohol in a separate step:

$$V_2O_5 + 2H_3PO_4 + H_2O \rightarrow 2VOPO_4 \cdot 2H_2O + H_2O$$

$$2VOPO_4 \cdot 2H_2O + EtCHOHMe \rightarrow 2VOHPO_4 \cdot 0.5H_2O + EtCOMe + 3H_2O$$
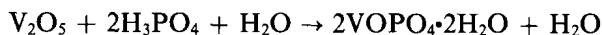
The *organic synthesis* usually provides the most active and selective catalysts [4,10,14,16,19]. All three methods may also lead to various hydrated vanadyl(IV) hydrogen phosphate phases, $VOHPO_4 \cdot nH_2O$ ($n = 0.5, 1, 2, 3,$ and 4), which are all precursors of the VPO catalysts. The precursor with $n = 0.5$ ($VOHPO_4 \cdot 0.5H_2O$) produces the best VPO catalysts [10]. Another phase, $VO(H_2PO_4)_2$, is observed when a considerable excess of phosphate is used in the organic synthesis ($P/V > 2$) [16]. The main differences observed in the VPO precursors obtained by various methods is the morphology of the $VOHPO_4 \cdot 0.5H_2O$ crystallites. The XRD patterns of $VOHPO_4 \cdot 0.5H_2O$ synthesized by aqueous and organic methods and, accordingly, referred to as *organic* and *aqueous* VPO precursors and catalysts are shown in Figure 1. These patterns indicate that organic precursors are less crystalline and preferentially expose the (001) planes [14], as manifested in a broader (001) reflection and its lower relative intensity as com-
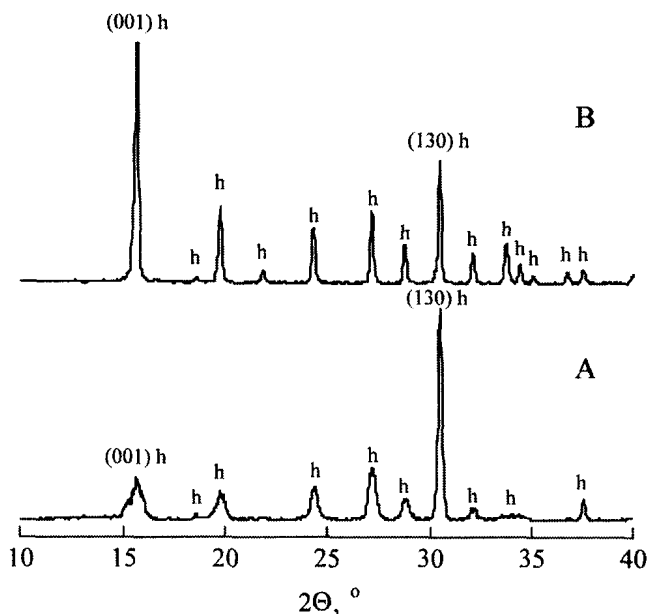
Figure 1　XRD patterns of the organic (A) and aqueous (B) precursors of VPO catalysts [63]. h = $VOHPO_4 \cdot 0.5H_2O$. Peak width: FWHM of (001) = 0.56 and 0.18°; FWHM of (130) = 0.18 and 0.22° in organic and aqueous precursors, respectively. Relative peak intensity: I(001)/I(130) = 0.20 and 1.95 in organic and aqueous precursors, respectively

pared to the intensity of the in-plane (130) reflection (Figure 1).

The morphology of organic precursors depends on many factors, e.g. (i) the nature of the solvent/reducing agent (an aliphatic or benzylic alcohol) [16, 19], (ii) the synthesis P/V ratio [16], (iii) the time and temperature of reduction [19], and (iv) the amount of water present during synthesis [16].

Currently only organic VPO catalysts are employed industrially in *n*-butane oxidation as the most active and selective. The following steps have been proposed in the formation of the $VOHPO_4 \cdot 0.5H_2O$ in organic medium [19]: (i) the formation of colloidal V_2O_5 at the water-alcohol interface, (ii) the dissolution of V_2O_5 through the formation of V^V-alcoholate species, (iii) the reduction of the dissolved V^V-alcoholate species in the liquid phase to solid V_2O_4, and (iv) the reaction of V_2O_4 with H_3PO_4 to form $VOHPO_4 \cdot 0.5H_2O$ at the solid-liquid interface. The type of aliphatic alcohol influences the temperature of reduction of V^V which is kinetically controlled and complete only at long reduction times upon addition of benzyl alcohol and orthophosphoric acid [19].

In the reduction by benzyl alcohol, many studies reported the formation of $VOHPO_4 \cdot 0.5H_2O$ platelets possessing stacking faults of the (001) planes seen in the preferential broadening of the (001) reflection. The stacking faults develop due to the trapping of alcohol molecules between the (001) layers of the precursor and their release during precursor transformation to $(VO)_2P_2O_7$ [4, 10, 16, 19]. The effect of the above synthesis parameters on the properties of $VOHPO_4 \cdot 0.5H_2O$ is to vary the exposure of the (001) plane, create the stacking fault strain in the crystallites and influence the degree of V^V reduction.

In both aqueous and organic syntheses, the $VOHPO_4 \cdot 0.5H_2O$ precursor has a P/V ratio higher than the stoichiometric value [10, 16, 19]. The maximum value corresponds to P/V = 1.1, while the excess phosphate remains in synthesis solution. The X-ray photoelectron (XPS) analysis indicates that the excess phosphate is localized at the surface of the vanadyl pyrophosphate catalysts (surface P/V = 1.5-3.0) [23].

The well-known redox chemistry of V^V provides important insights into the mechanism of the $VOHPO_4 \cdot 0.5H_2O$ precursor formation in organic medium. Waters and Littler [24] have shown that most V^V reductions proceed via a free-radical mechanism where complexation of V^V to alcohol precedes the one-electron transfer step, i.e. an inner sphere electron transfer. Waters and Littler [24] proposed ternary tetrahedral complex formation between VO_2^+, H_3O^+ and R_2CHOH to yield $[V(OH)_3OHCHR_2]^{2+}$ and observed the following kinetic expression

$$-d[V^V]/dt = k[R_2CHOH][VO_2^+][H_3O^+]$$

corresponding to slow decomposition of this species to V^{IV} and an alcohol radical, $R_2C^\bullet\text{-}OH$. The formation of the protonated complex should be assisted by the more acidic medium which was observed experimentally in numerous studies [24-26]. The inertness of simple tertiary alcohols toward V^V indicated that the α-C-H bond is involved in the reaction which was confirmed by measuring the primary isotope effect produced by deuterium substitution at this position in cyclohexanol [24]. A mechanism involving cyclic transfer of the α-H

atom to a coordination sphere of the metal ion has been proposed:

$$VO_2^+ + H_3O^+ \rightleftharpoons [V(OH)_3]^{2+} \xrightarrow{R_2CHOH} [R_2C\text{-}\underset{H}{\overset{H\quad OH}{|}}V(OH)_2]^{2+} \xrightarrow{\text{slow}}$$

$$\xrightarrow{} [R_2\overset{\bullet}{C}\text{-}\underset{H}{O}\rightarrow V(OH)_2H_2O]^{2+} \xrightarrow{} R_2\overset{\bullet}{C}OH + VO^{2+} + 2H_2O$$
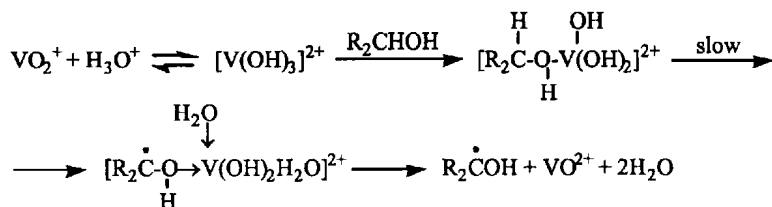
This mechanism shows that the V^V reduction during the VPO precursor synthesis is slow at low H_3O^+ concentration. The rate of reduction is slow even in the presence of anhydrous H_3PO_4, since $[H_3O^+]$ is low in the absence of water. The reaction is likely autocatalytic: the water evolved during the reduction is protonated and the resultant H_3O^+ accelerates the reaction rate.

Rocek and Aylward [27] used substituted cyclobutanols as a probe into the mechanism of V^V reduction by alcohols. Oxidation of cyclobutanols is a widely accepted method for discerning one- and two-electron processes, as they lead to cyclobutanones and γ-hydroxyaldehydes, respectively [28-30]. Rocek and Aylward [27] observed the formation of γ-hydroxyaldehydes in V^V reductions providing evidence of a one-electron process. The V^V oxidation of cyclobutanols is first order in both the cyclobutanols and the protonated monomeric HVO_2^+ (aq.) species. HVO_2^+ (aq.) is a stronger oxidant than VO_2^{2+} (aq.), and at the acidic conditions employed in these oxidations, V^V was predominantly in its monomeric form (HVO_2^+), despite its pronounced tendency toward the formation of polymeric ions [31]. Methyl cyclobutyl ether was found to be 10^4 times less reactive than cyclobutanol. This striking difference in reactivity indicated that the OH bond plays a vital role in the oxidation process and is broken either prior to or during the rate-determining step, as explained by formation of an ester of vanadic acid intermediate suggested as $ROV(OH)_2(OH_2)_n^{2+}$ ($n = 1, 2,$ or 3).

Tracey and Gresser [32] confirmed spontaneous formation of vanadate esters in aqueous solutions of alcohols in ^{51}V NMR spectra (pH = 7-11, 1-50 mM, 328K) where the vanadate occurs as the tetrahedral mono- or diprotonated anions, HVO_4^{2-} and $H_2VO_4^-$ denoted as V_i, dimeric ($HO_3VOVO_3H^{2-}$ or V_2), and tetrameric ($H_4V_4O_{14}^{4-}$ or V_4) species. The complexity of esterification of vanadate arises in part from the ability of vanadate (VO_4^{3-}) to undergo protonation and oligomerization as pH and concentration are changed [31,33,34]. Tracey and Gresser showed that vanadate complexes with monodentate hydroxylic ligands are tetrahedral analogs of phosphate esters. Equilibrium constants for the formation of monoanionic alkyl vanadate esters from V_i monoanion and alcohols, $K_f = [ROVO_3H^-]/[(H_2VO_4^-][ROH])$, are about 0.2 M^{-1}, and relatively insensitive to the pK_a of the alcohol and to whether the alcohol is primary, secondary, or tertiary [35-38]. Since the pK_a values of V_i and alkylvanadates are above 8.0, this K_f value can be used to estimate the concentration of a given vanadate ester in solution at a neutral pH containing known concentrations of V_i and alcohol. In studies of V_i in aqueous methanol Tracey and co-workers [38] found that methyl esters of *divanadate* can also form sponta-

neously with equilibrium constants similar to those for formation of esters of monovanadate: $V_2 + MeOH \rightarrow V_2(OMe) + H_2O$, $K = 3.0 \ M^{-1}$.

Gresser *et al.* [39] observed formation of mixed anhydrides of vanadate with phosphate and pyrophosphate in aqueous solutions by ^{51}V NMR, which may be considered as *molecular precursors of vanadium phosphate phases*. The formation of the mixed anhydrides was in fact more favorable than that of phosphate anhydrides (i.e. pyrophosphate) by more than 10^6-fold in the K_f for the phosphovanadate as compared to pyrophosphate at neutral pH. Formation of the divanadate species (V_2) was 10^8 times more favored over formation of pyrophosphate. The reasons for the preferred formation of phosphovanadates may have to do with an interaction of the lone pairs of electrons on the bridging oxygen atom with orbitals on the adjacent vanadium and phosphorus atoms. If this occurred, it would cause the bridging oxygen to be more *sp*-like than sp^3, with the result that the P-O-V or V-O-V bond angle in the anhydride would be larger than the P-O-P angle in the pyrophosphate. If the V-O-V and P-O-V angles are large, then the corresponding anhydrides in contrast to the pyrophosphate [40] may not be able to chelate Mg^{2+} which has been confirmed experimentally [41].

Some of the ways the vanadate esters and phosphovanadates [32-39] may be involved in the reduction of V^V during the $VOHPO_4 \cdot 0.5H_2O$ precursor formation are:

A.   Redox decomposition of monoalkyl esters of monomeric vanadate via a mechanism similar to that of Waters and Littler [24]. In this case, free radical species will be generated which can be detected by an ESR spin trapping technique.

B.   Redox decomposition of monoalkyl ester of dimeric vanadate, $ROVO_2$-O-VO_3^{3-}, accompanied by two rapid successive one-electron transfers. Then, no free radical species are expected, and the products should be the carbonyl compound and VO^{2+}. This mechanism has not yet been established for vanadate oxidations.

C.   Redox decomposition of monoalkyl esters of phosphovanadate, $[ROV^VO_2$-O-$PO_3H]^{2-}$, similar to case A. However, in this case the redox decomposition may lead to $[V^{IV}O(H_2O)_4OPO_3H]$ species which precedes the formation of $VOHPO_4 \cdot 0.5H_2O$ precursor. The $[V^{IV}O(H_2O)_4OPO_3H]$ species may be detected during early stages of V^V reduction by ESR.

3   Thermal Activation of $VOHPO_4 \cdot 0.5H_2O$ Precursor

A number of crystalline VPO phases were observed during the transformation of the $VOHPO_4 \cdot 0.5H_2O$ precursor to the active VPO catalyst [11, 12] depending on:

• the temperature, time, and atmosphere of activation;
• the morphology of the precursor;
• the P/V ratio in the precursor; and
• the presence defects in the structure.

Two different activation procedures are generally reported in the scientific and patent literature:

- Activation in an oxygen-free atmosphere at T > 673K, followed by introduction of the reactant mixture of *n*-butane in air. $VOHPO_4 \cdot 0.5H_2O$ transforms quantitatively to poorly crystalline $(VO)_2P_2O_7$ during the first step [16], which can be partially oxidized to V^V orthophosphates after the introduction of the reactant mixture [13].
- Calcination in air at T < 673K, after which the reactant mixture is introduced [15, 16, 23].

As the $VOHPO_4 \cdot 0.5H_2O$ precursor is heated, the trapped alcohol molecules are released, which creates structural defects, microcracks and increases the surface area. The precursor first transforms into an amorphous phase [15, 23], which can be further dehydrated to crystalline $(VO)_2P_2O_7$ and partially oxidized to V^V orthophosphates once the reactant mixture is introduced. Excess phosphate present in the precursor stabilizes $(VO)_2P_2O_7$ against overoxidation in oxygen-containing atmosphere [13]. The *in situ* Raman spectroscopy provided insights into the nature of the transformation of the model organic $VOHPO_4 \cdot 0.5H_2O$ precursor [42]. When the precursor phase was heated in an inert He atmosphere, a continuous loss of local order was observed up to 724K. At that temperature, fingerprint Raman bands of $VOHPO_4 \cdot 0.5H_2O$ were no longer visible, and instead weak features corresponding to poorly crystalline $(VO)_2P_2O_7$ emerged. The *in situ* spectra suggested that these two phases did not coexist during the precursor transformation in inert atmosphere. Similar observations were made during the precursor transformation in reactive *n*-butane-air environment. The precursor is completely transformed into a mixture of δ-$VOPO_4$ and $(VO)_2P_2O_7$ at 708K. The redox environment leads to partial oxidation of vanadyl(IV) species into a V(V) orthophosphate. The presence of V(V) orthophosphate is usually responsible for higher activity and lower selectivity of these catalysts as compared to the fresh catalysts activated in inert atmosphere. It is interesting that the transformation proceeds via formation of an amorphous VPO intermediate regardless of the gas environment, and that $VOHPO_4 \cdot 0.5H_2O$ and $(VO)_2P_2O_7$ phases are not observed simultaneously during the transformation. Figure 2 shows the different phase transformations in the VPO system [43]. Xue and Schrader further examined the VPO phase transformations using the *in situ* Raman spectroscopy [44]. They found that $(VO)_2P_2O_7$ experienced a structural disorder during prolonged exposure to water vapor at elevated temperatures which resulted in the V-O-P bond breaking, the loss of phosphate and the appearance of bulk vanadium oxide.

Electron microscopy studies [16, 19, 45] have shown that $(VO)_2P_2O_7$ maintains the morphology of the precursor. The XRD data are also consistent with the broadening of the interlayer spacing reflections in both $VOHPO_4 \cdot 0.5H_2O$ ((001) vs. the in-plane (130) reflection) and $(VO)_2P_2O_7$ ((200) vs. the in-plane (024) reflection) shown in Figure 1 and 3. Based on these observations as well as on close structural analogies of the two phases Bordes *et al.* [43] proposed that the transformation of $VOHPO_4 \cdot 0.5H_2O$ to $(VO)_2P_2O_7$ is topotactic, i.e. it proceeds
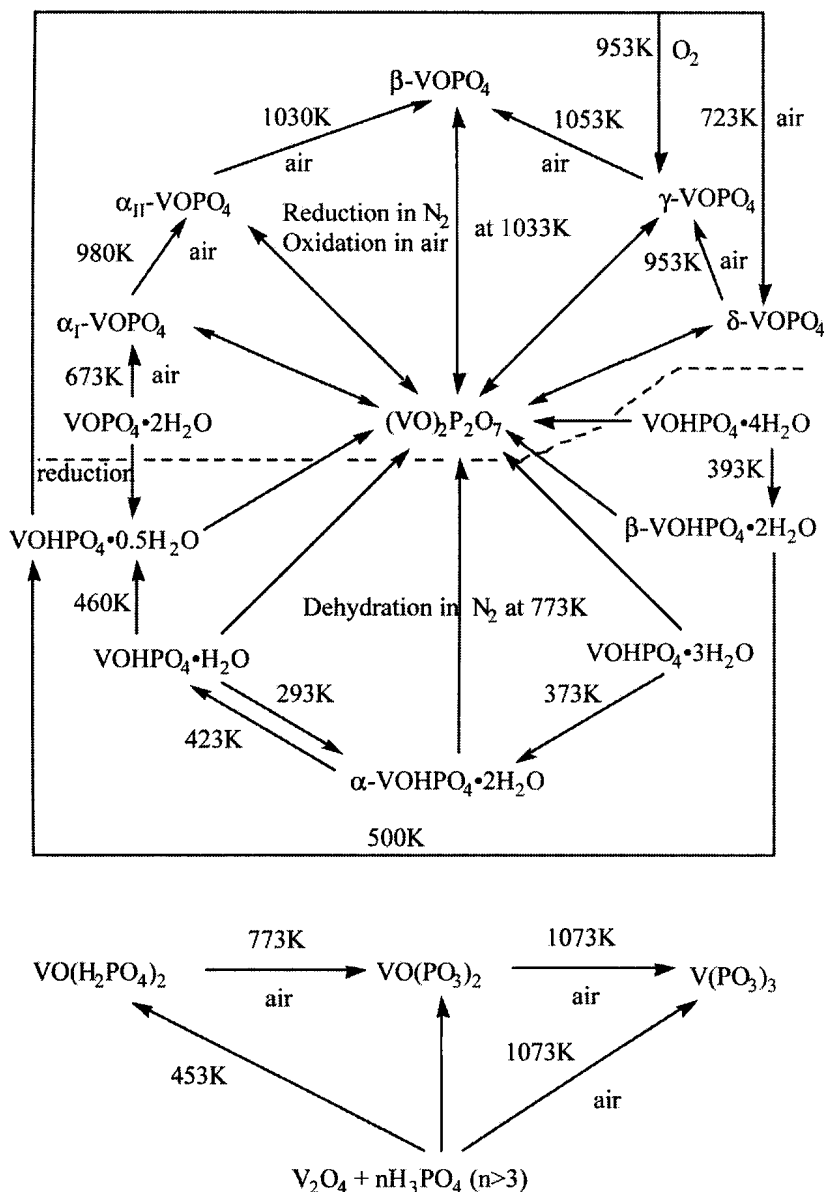
Figure 2   *Phase transformations in the VPO system [43]. Dashed lines separate the reversible redox transformations to (VO)$_2$P$_2$O$_7$ (top) from irreversible dehydrations (bottom)*

with the preservation of the V-O-P connectivity.

Thompson *et al.* [46] analyzed symmetries of the two structures and suggested that this transformation is unlikely topotactic. Their suggestion is in agreement with the observation of an amorphous intermediate phase during the transform-